TU–698
October 2003

Renormalon Cancellation and Perturbative QCD Potential as a Coulomb+Linear Potential*

Y. Sumino

Department of Physics, Tohoku University
Sendai, 980-8578 Japan

Abstract

Recently evidence has been found that the perturbative QCD potential agrees well with phenomenological potentials and lattice computations of the QCD potential. We review the present status of the perturbative QCD potential and theoretical backgrounds. We also report our recent analysis which shows analytically, on the basis of renormalon dominance picture, that the perturbative QCD potential quickly "converges" to a Coulomb-plus-linear form. The Coulomb-plus-linear potential can be computed systematically as we include more terms of the perturbative series; up to three-loop running (our current best knowledge), it shows a convergence towards lattice results. e.g. At one-loop running, the linear potential is σr with $\sigma = (2\pi C_F/\beta_0)\Lambda^2_{\overline{\rm MS}}$.

*Invited talk given at the "International Conference on Color Confinement and Hadrons in Quantum Chromodynamics (Confinement 2003)", Riken, Tokyo, 21–24 July 2003.

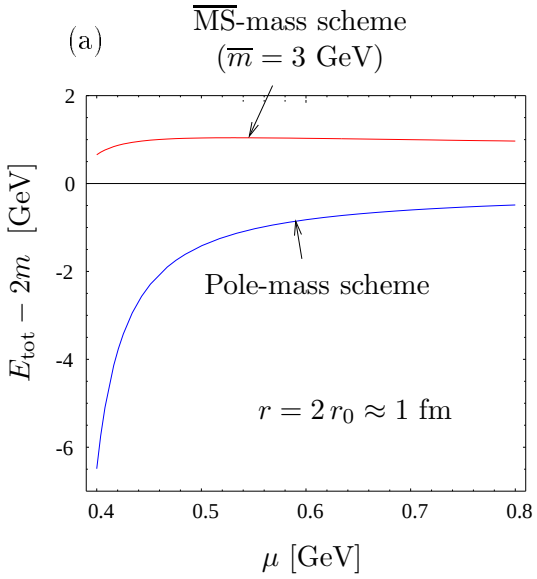

(b)

Scheme	$E_{\rm tot}(2r_0)$ at $\mu = 0.53$ GeV		
	$\mathcal{O}(\alpha_S)$	$\mathcal{O}(\alpha_S^2)$	$\mathcal{O}(\alpha_S^3)$
Pole mass	-0.14	-0.26	-0.75
$\overline{\rm MS}$ mass	$+1.20$	-0.14	-0.022

Figure 1: (a)Scale dependences of $E_{\rm tot}(r)$ at $r = 2r_0 \approx 1$ fm, in the pole-mass and $\overline{\rm MS}$-mass schemes. ($\overline{m} \equiv m_{\overline{\rm MS}}(m_{\overline{\rm MS}}) = 3$ GeV) (b) Perturbative series of $E_{\rm tot}(r)$ at $r = 2r_0$, and at $\mu = 0.53$ GeV determined from $\partial E_{\rm tot}/\partial\mu = 0$ in (a) ($\overline{\rm MS}$-mass scheme).

1 Introduction

In this article, we review the perturbative QCD predictions of the QCD potential for a static quark-antiquark ($Q\bar{Q}$) pair, in the distance region relevant to the bottomonium and charmonium states, namely, 0.5 GeV^{-1}(0.1 fm) $\lesssim r \lesssim$ 5 GeV^{-1}(1 fm).

Several years ago, the perturbative prediction of the QCD potential became much more accurate in this region. There were two important developments: (1) The complete $O(\alpha_S^3)$ corrections to the QCD potential have been computed [1]; also the relation between the quark pole mass and the $\overline{\rm MS}$ mass has been computed up to $O(\alpha_S^3)$ [2]. (2) A renormalon cancellation was discovered [3] in the total energy of a static $Q\bar{Q}$ pair*, $E_{\rm tot}(r) \equiv 2m_{\rm pole} + V_{\rm QCD}(r)$. Consequently, convergence of the perturbative series of $E_{\rm tot}(r)$ improves drastically, if it is expressed in terms of the quark $\overline{\rm MS}$ mass instead of the pole mass.

Let us demonstrate the improvement of accuracy of the perturbative prediction for $E_{\rm tot}(r)$ up to $O(\alpha_S^3)$, in the case without light quark flavors ($n_l = 0$). In Fig. 1(a), we fix r to be $2r_0 \approx 1$ fm as an extreme long-distance case† and show the renormalization-scale (μ) dependence of $E_{\rm tot}(r = 2r_0)$. We see that $E_{\rm tot}$ is much less scale dependent when we use the $\overline{\rm MS}$ mass instead of the pole mass. Fig. 1(b) compares the convergence behaviors of the perturbative series of $E_{\rm tot}$ for the same r and when μ is fixed to the value where $E_{\rm tot}$ becomes least sensitive to variation of μ (minimal-sensitivity scale). If we use the pole mass, the series is divergent, whereas for the $\overline{\rm MS}$ mass, the series is convergent.‡ In fact, we observe qualitatively the same features at different r and for different number of light quark flavors n_l. Generally, at smaller r, $E_{\rm tot}(r)$ becomes less μ-dependent and more convergent.

The aim of this paper is to study properties of $E_{\rm tot}(r)$, given the much more accurate prediction

*By "static", we mean that the kinetic energies of Q and $\bar{Q}$ are neglected.

†$r_0 \approx 0.602\,\Lambda_{\overline{\rm MS}}^{-1}$ [4] represents the Sommer scale. It is translated to physical unit following the convention of lattice calculations in the quenched approximation: $r_0 \approx 0.5$ fm.

‡When the series is convergent ($\overline{\rm MS}$-mass scheme), μ-dependence decreases as we include more terms of the perturbative series into $E_{\rm tot}(r)$, whereas when the series is divergent (pole-mass scheme), μ-dependence does not decrease with increasing order.

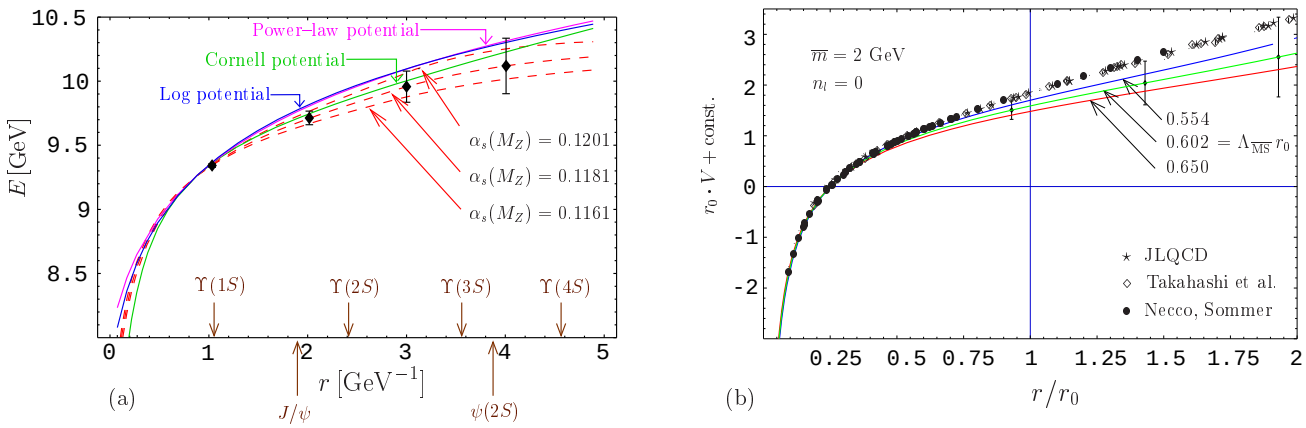

Figure 2: (a) Comparison between $E_{\rm tot}(r)$ and typical phenomenological potentials [6]. Arrows at the bottom show the r.m.s. radii of the heavy quarkonium states. (b) Comparison between $E_{\rm tot}(r)$ and lattice computations of the QCD potential [7].

as compared to several years ago. In Sec. 2 we examine $E_{\rm tot}(r)$ up to $O(\alpha_S^3)$. Sec. 3 provides our present theoretical understanding based on renormalon dominance picture and operator-product-expansion (OPE). We show that the perturbative QCD potential "converges" to a Coulomb+linear potential in Sec. 4. Conclusions are given in Sec. 5.

2 $E_{\rm tot}(r)$ up to $O(\alpha_S^3)$

The most solid part of our study is an examination of the perturbative predictions of $E_{\rm tot}(r)$ up to $O(\alpha_S^3)$, through comparisons with phenomenological potentials and with lattice computations of the QCD potential.

In Fig. 2(a), $E_{\rm tot}(r)$ is compared with typical phenomenological potentials. Since the latter are determined from the heavy quarkonium spectra, we choose realistic values for the input parameters of $E_{\rm tot}(r)$: $\overline{m}_b = 4.190$ GeV; $n_l = 4$ with $\overline{m}_u = \overline{m}_d = \overline{m}_s = 0$ and $\overline{m}_c = 1.243$ GeV for the light quarks in internal loops; $\mu = \mu(r)$ is fixed by either $\partial E_{\rm tot}/\partial\mu = 0$ or $|E^{(3)}_{\rm tot}| =$ minimum, but both prescriptions lead to almost same values of $E_{\rm tot}(r)$. See [5, 6] for details. We see that $E_{\rm tot}(r)$ corresponding to the present values of the strong coupling constant (dashed lines) agree well with the phenomenological potentials within estimated perturbative uncertainties (indicated by error bars). We also note that the agreement is lost quickly if we take $\alpha_S(M_Z)$ outside of the present world-average values, so that the agreement is unlikely to be accidental.

In Fig. 2(b), $E_{\rm tot}(r)$ is compared with the recent lattice computations of the QCD potential in the quenched approximation. Accordingly we set $n_l = 0$ in $E_{\rm tot}(r)$. We take $\overline{m} = 2$ GeV, which stabilizes the perturbative prediction up to largest r. The scale $\mu = \mu(r)$ is fixed in the same way as in Fig. 2(a). See [7] for details. The three solid lines in Fig. 2(b) represent the same perturbative prediction for $E_{\rm tot}(r)$; there is an error in the relation between $\Lambda_{\overline{\rm MS}}$ and the lattice scale, and the three lines represent the error band of this relation $\Lambda_{\overline{\rm MS}} r_0 = 0.602(48)$ as given by [4]. Taking this uncertainty into account and also uncertainties of the perturbative prediction (error bars), we observe a good agreement between $E_{\rm tot}(r)$ and lattice results.

In fact, by now several works have confirmed the agreements [5, 8, 6, 9, 7]. Although details depend on how the renormalon in the QCD potential is cancelled, qualitatively the same conclusions were drawn, i.e. perturbative predictions become accurate and agree with phenomenological

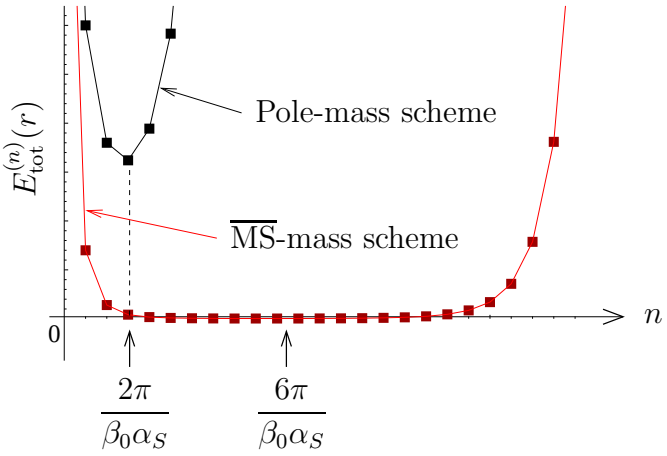

Figure 3: Schematic diagram showing n-dependence of $|V^{(n)}_{\beta_0}(r)|$ (or $|E^{(n)}_{\rm tot}(r)|$ in the pole-mass scheme) [black points] and that of $|E^{(n)}_{\rm tot}(r)|$ in the $\overline{\rm MS}$-mass scheme [red points].

potentials/lattice results up to much larger r than before. In particular, in the differences between the perturbative predictions and phenomenological potentials/lattice results, a linear potential of order $\Lambda^2_{\rm QCD} r$ at short distances $r \ll \Lambda^{-1}_{\rm QCD}$ was ruled out numerically.

3 Theoretical Backgrounds

We would like to understand why the perturbative predictions of $E_{\rm tot}(r)$ behave in the way we observed in the previous sections. In this section, we review our current theoretical understanding.

3.1 Perturbative uncertainties: Leading-order renormalon

The nature of the perturbative series of $V_{\rm QCD}(r)$ and $E_{\rm tot}(r)$, including their uncertainties, can be understood within the argument based on renormalons. This argument gives certain estimates of higher-order corrections in perturbative QCD, and empirically it gives good estimates even at relatively low orders of perturbative series.

According to the renormalon argument, the perturbative series of $V_{\rm QCD}(r)$ (or $E_{\rm tot}(r)$ in the pole-mass scheme) behaves as depicted in Fig. 3 [black points]; see e.g. [10]. Namely, the series shows apparent convergence up to order $\alpha_S^{n_0}$ with $n_0 \approx 2\pi/(\beta_0\alpha_S)$. Beyond this order, the series diverges. Due to the divergence (the series is an asymptotic series), there is a limitation to the achievable accuracy of the perturbative prediction. It can be estimated by the size of the terms around the minimum, $O(\alpha_S^{n_0})$; this gives an uncertainty for $V_{\rm QCD}(r)$ of order $\Lambda_{\rm QCD} \sim 300$ MeV [11].

To obtain the above behavior, we may use, for instance, the "large-β_0 approximation" [12] to estimate the higher-order corrections. The order α_S^{n+1} term of $V_{\rm QCD}(r)$ for $n \gg 1$ is estimated as

$$V^{(n)}_{\beta_0}(r) \sim -\frac{2C_F\alpha_S(\mu)}{\pi}\,\mu\,e^{5/6} \times \left(\frac{\beta_0\alpha_S(\mu)}{2\pi}\right)^n \times n!, \tag{1}$$

where $C_F = 4/3$ is a color factor and $\beta_0 = 11 - 2n_l/3$ is the 1-loop coefficient of the beta function. From this expression, it is easy to obtain the behavior of the series as explained above.

It is important to note that Eq. (1) is independent of r. Although $V^{(n)}_{\beta_0}(r)$ is dependent on r, the leading part in the large n limit is independent of r. This feature can be verified in Fig. 4(a):

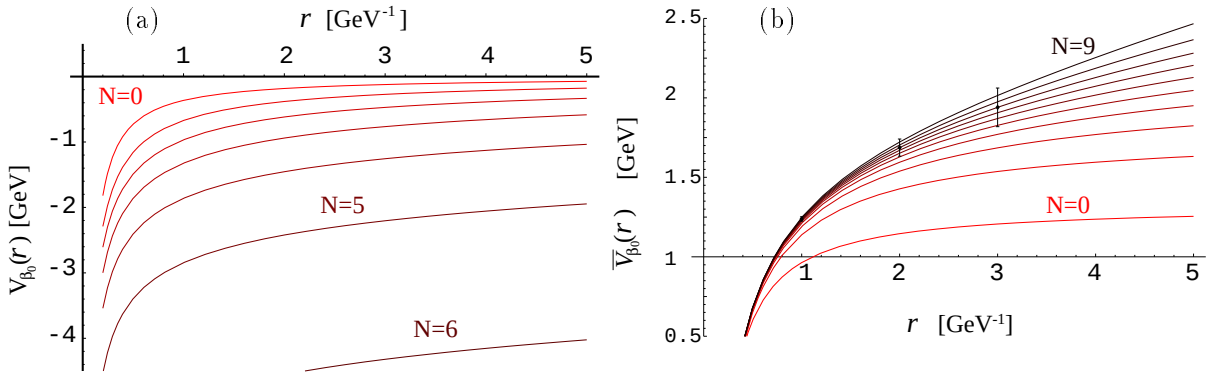

Figure 4: $V_{\beta_0}(r)$ truncated at $O(\alpha_S^{N+1})$ term, $\sum_{n=0}^{N} V_{\beta_0}^{(n)}(r)$. We set $\mu = 2.49$ GeV, $n_l = 4$ and $\alpha_S(\mu) = 0.273$. (a) Before cancellation of the leading-order renormalon. (b) After cancellation of the leading-order renormalon. Note that the vertical scales are different in two figures. (The figures are taken from [5].)

As we include more terms of the perturbative series of $V_{\rm QCD}(r)$ (in the large-β_0 approximation), there are large corrections to the potential, which shift the potential almost r-independently. Furthermore, one sees no sign of convergence of the perturbative series in the range of r we are interested in.

3.2 Renormalon cancellation and its implications

As already stated, the leading-order renormalon uncertainty in the QCD potential gets cancelled in the $Q\bar{Q}$ total energy, $E_{\rm tot}(r) = 2m_{\rm pole} + V_{\rm QCD}(r)$, if we use the $\overline{\rm MS}$ mass. As seen above, the leading-order renormalon is independent of r, hence, it can be absorbed by a redefinition of the quark mass. The pole mass is expressed in terms of the $\overline{\rm MS}$ mass as a perturbative series, $m_{\rm pole} = \overline{m}\,(1 + c_1\alpha_S + c_2\alpha_S^2 + \cdots)$. The leading part of this series at large orders takes the same form as Eq. (1) but in opposite sign and with half magnitude [13]. As a result, the leading-order renormalon is cancelled* in $E_{\rm tot}(r)$ and its perturbative series behaves as [3]

$$E_{\rm tot}^{(n)}(r) \sim \text{const.} \times r^2 \times \left(\frac{\beta_0\alpha_S(\mu)}{6\pi}\right)^n \times n! \tag{2}$$

at large n. As compared to $V_{\beta_0}(r)$, the series converges faster and up to larger order, $n \approx 6\pi/(\beta_0\alpha_S)$, but beyond this order again the series diverges; see Fig. 3. An uncertainty of this perturbative series can be estimated from the size of the terms around the minimum, which gives $\delta E_{\rm tot}(r) \sim \Lambda_{\rm QCD} \times (r\Lambda_{\rm QCD})^2$. Thus, at distances $r \lesssim \Lambda_{\rm QCD}^{-1}$, the uncertainty becomes smaller than the original uncertainty $\delta V_{\rm QCD}(r) \sim \Lambda_{\rm QCD}$. In fact, the error bars in Figs. 2(a,b) represent $\pm\frac{1}{2}\Lambda^3 r^2$ with $\Lambda = 300$ MeV. The agreement of $E_{\rm tot}(r)$ and phenomenological potentials/lattice results holds within this uncertainty.

A significant improvement of convergence can be seen by comparing Figs. 4(a) and (b), where higher-order corrections are estimated using the large-β_0 approximation. Moreover, in Fig. 4(b) we see that the higher-order corrections make the potential steeper at large r, as compared to the tree-level ($N = 0$) Coulomb potential. In fact, due to this very feature, agreements between $E_{\rm tot}(r)$ and phenomenological potentials/lattice results were observed in Sec. 2. We may understand the

*For the complete cancellation of the leading behavior Eq. (1), one needs to expand $V_{\rm QCD}(r)$ and $m_{\rm pole}$ in the *same* coupling constant $\alpha_S(\mu)$. This is somewhat involved technically, since usually $V_{\rm QCD}(r)$ and $m_{\rm pole}$ are expressed in terms of different coupling constants; see [5–7].

reason as follows. Let us define a strong coupling constant $\alpha_F(\mu)$ from the interquark force:

$$F(r) \equiv -\frac{d}{dr} V_{\rm QCD}(r) \equiv -C_F \frac{\alpha_F(1/r)}{r^2}. \tag{3}$$

Since the leading-order renormalon in $V_{\rm QCD}(r)$ is r-independent, it is *killed* upon differentiation by r. $\alpha_F(1/r)$ grows at infrared (IR) due to the running (the first two coefficients of the β-function are universal), which makes $|F(r)|$ stronger than the Coulomb force at large r. This means that $V_{\rm QCD}(r)$, after cancelling the leading-order renormalon, becomes steeper than the Coulomb potential. Within perturbative QCD, arguments based on $F(r)$ are much more secure than those based on $V_{\rm QCD}(r)$ in the range of r of our interest. See [5, 8] for details.

Conventionally, theoretical calculations of the energy of a heavy $Q\bar{Q}$ boundstate closely followed that of a QED boundstate such as positronium: it starts from the natural picture that, when an electron and a positron are at rest and far apart from each other, they tend to be free particles and the total energy of the system is given by the sum of the energies of the two particles (pole masses); as the electron and positron approach each other, the energy of the system decreases due to the negative potential energy, so that the total energy of the boundstate is given as the sum of the pole masses minus the binding energy. Applying the same description to the energy of a $Q\bar{Q}$ system, however, is not natural, because when Q and $\bar{Q}$ are far apart from each other, the free quark picture is not good. As a result, the perturbative expansion of the boundstate energy turns out to be poorly convergent, due to the contributions from IR gluons with wave-lengths of order $\Lambda_{\rm QCD}^{-1}$. On the other hand, intuitively we expect that there should be a way to calculate the boundstate energy in which the contributions of IR gluons can be mostly eliminated. This is because when the boundstate size is sufficiently smaller than $\Lambda_{\rm QCD}^{-1}$, IR gluons cannot resolve the color charges of the constituent particles, so that they decouple from this color-singlet system. Such a calculation is possible if we use a quark mass (e.g. $\overline{\rm MS}$ mass), into which only contributions from short wave-length gluons to the quark self-energy are absorbed (renormalized).

According to the renormalon argument (in the large-β_0 approximation), the QCD potential and the pole mass are roughly given by

$$V_{\rm QCD}(r) \approx -\int \frac{d^3\vec{q}}{(2\pi)^3}\, e^{i\vec{q}\cdot\vec{r}}\, C_F \frac{4\pi\alpha_S(q)}{q^2}, \tag{4}$$

$$m_{\rm pole} \approx \overline{m} + \frac{1}{2}\int_{q \lesssim \overline{m}} \frac{d^3\vec{q}}{(2\pi)^3}\, C_F \frac{4\pi\alpha_S(q)}{q^2}, \tag{5}$$

where $q = |\vec{q}|$ and $\alpha_S(q)$ is (essentially) the one-loop running coupling constant.[†] It follows that qualitatively the $Q\bar{Q}$ total energy can be expressed as [14, 5][‡]

$$E_{\rm tot}(r) \simeq 2\overline{m} + \int_{r^{-1} \lesssim q \lesssim \overline{m}} \frac{d^3\vec{q}}{(2\pi)^3}\, C_F \frac{4\pi\alpha_S(q)}{q^2}. \tag{6}$$

It shows that the energy is mainly composed of (i) the $\overline{\rm MS}$ masses of Q and $\bar{Q}$, and (ii) the self-energies of Q and $\bar{Q}$ originating from gluons whose wavelengths are shorter than the size of the

[†]The large-β_0 approximation is essentially a resummation of gluon vacuum polarization, which effectively changes the coupling constant $\alpha_S(\mu)$ to the one-loop running coupling constant, $\alpha_S(q) = \alpha_S(\mu)/[1-\beta_0\alpha_S(\mu)\log(\tilde{\mu}/q)/(2\pi)]$, where $\tilde{\mu} = e^{5/6}\mu$ in order to account for the non-logarithmic term of the vacuum polarization.

[‡]IR part of $V_{\rm QCD}(r)$ in Eq. (4) is cancelled against that of $2m_{\rm pole}$, since $e^{i\vec{q}\cdot\vec{r}} \sim 1$ at $q \ll 1/r$. On the other hand, at $q \gg 1/r$, $e^{i\vec{q}\cdot\vec{r}}$ is highly oscillatory and contributions to $V_{\rm QCD}(r)$ from this region are suppressed.

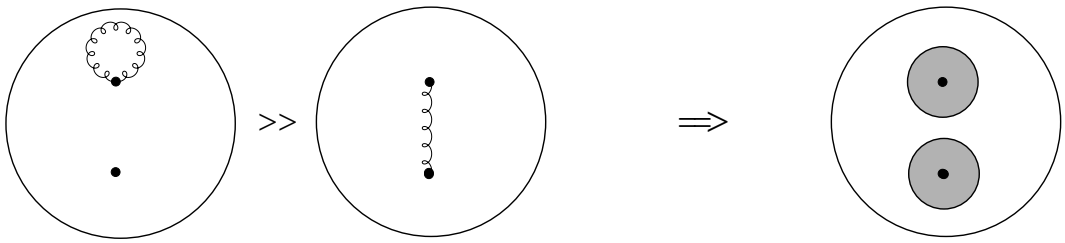

Figure 5: Total energy of a heavy $Q\bar{Q}$ pair is mainly composed of (i) the $\overline{\rm MS}$ masses of Q and $\bar{Q}$, and (ii) the contributions from gluons with wavelengths $1/\overline{m} \lesssim \lambda_g \lesssim r$. In (ii) the self-energies of Q and $\bar{Q}$ dominate over the potential energy between the two particles.

system and longer than those absorbed into (i), i.e. $1/\overline{m} \lesssim \lambda_g \lesssim r$. See Fig. 5. Thus, IR gluons ($\lambda_g > r$) have decoupled from Eq. (6). If $\alpha_S(q)$ were a constant (non-running), $E_{\rm tot}(r)$ would be a Coulomb potential. Due to the running of $\alpha_S(q)$, however, there is a large positive contribution in Eq. (6) as r increases and gets closer to $\Lambda_{\rm QCD}^{-1}$. This gives a microscopic description for how $E_{\rm tot}(r)$ becomes steeper than the Coulomb potential at large r: It is the rapid growth of the self-energies (ii) as more IR gluons couple to this system with increasing r. — Again it stems from the *running* of the strong coupling constant.

3.3 Consistency with operator-product-expansion

An OPE of the QCD potential can be performed within the effective field theory "potential-NRQCD" [15]. The dynamical degrees of freedom in this effective theory have only very soft scale, where typical momenta are $k \ll 1/r$. Higher momentum scales are integrated out and the effective interactions are generally non-local in space but local in time (potentials). In this framework, IR part of perturbative QCD calculations is factorized and absorbed into matrix elements of operators. A factorization scale $\mu_{\rm fac}$ is set to satisfy $\Lambda_{\rm QCD} \ll \mu_{\rm fac} \ll 1/r$. Then the total energy of a static $Q\bar{Q}$ pair is given by [16, 9]

$$E_{\rm tot}(r) = 2m_{\rm pole} + V_{\rm PT}(r;\mu_{\rm fac}) + \delta E_{\rm US}(r;\mu_{\rm fac}), \tag{7}$$

$$\delta E_{\rm US} = r^2 \times \frac{4\pi\alpha_S}{18} \int_0^\infty dt\, e^{-it(V_O - V_S)} \left\langle \vec{E}^a(t)\phi(t,0)_{ab}\vec{E}^b(0) \right\rangle (\mu_{\rm fac}) + \cdots \tag{8}$$

The perturbative potential $V_{PT}(r;\mu_{\rm fac})$ is now free from renormalons. The renormalons are absorbed into $2m_{\rm pole}$ and $\delta E_{\rm US}(r;\mu_{\rm fac})$. In the leading-order of multipole expansion, $\delta E_{\rm US}$ is proportional to r^2, as shown above. This is consistent with our observation in Sec. 2. Namely, the agreement between $E_{\rm tot}(r)$ and phenomenological potentials/lattice results holds within the $O(\Lambda_{\rm QCD}^3 r^2)$ renormalon uncertainty, while a difference of order $\Lambda_{\rm QCD}^2 r$ between them was ruled out (numerically) at distances $r \ll \Lambda_{\rm QCD}^{-1}$. According to OPE, indeed such a (linear) difference is not allowed theoretically, since there exists no operator that can absorb a linear potential.

4 Pert. QCD Potential as a Coulomb+Linear Potential

The observations and theoretical arguments in Secs. 2,3 indicate that the perturbative prediction of $E_{\rm tot}(r)$ takes a Coulomb+linear form (up to an r-independent constant) in the range $r \lesssim \Lambda_{\rm QCD}^{-1}$, as represented by a typical phenomenological potential. We would like to substantiate this claim

analytically. Since the uncertainty of the perturbative prediction is of order r^2, there is a possibility that $E_{\rm tot}(r)$ is predictable up to order r (linear) term at $r \lesssim \Lambda_{\rm QCD}^{-1}$ within perturbative QCD.

Nevertheless, one immediately comes up with counter arguments: (1) A finite-order perturbative prediction of $E_{\rm tot}(r)$ *cannot* be expressed in a Coulomb+linear form. This is because the perturbative QCD potential up to $O(\alpha_S^N)$ has a form

$$V_N(r) = -C_F \frac{\alpha_S(\mu)}{r} \times \sum_{n=0}^{N-1} \alpha_S(\mu)^n \, P_n(\log \mu r), \tag{9}$$

where $P_n(L)$ denotes an n-th degree polynomial of L. Therefore, as $r \to \infty$, $V_N(r) \to 0$, i.e. the tangent is zero, and there is no linear potential. (2) From dimensional analysis, the coefficient of a linear potential should be non-analytic in α_S, i.e. of order $\Lambda_{\rm QCD}^2 \sim \mu^2 \exp[-4\pi/(\beta_0 \alpha_S)]$. Therefore, it should vanish at any order of perturbative expansion. We will come back to these arguments later.

Since we observed a numerical agreement between $E_{\rm tot}(r)$ up to $O(\alpha_S^3)$ and a Coulomb-plus-linear potential, it would be interesting to examine how $E_{\rm tot}(r)$ up to $O(\alpha_S^N)$ or $V_N(r)$ will behave at large orders, $N \to \infty$. For this analysis, we need (a) some estimates of higher-order terms of $V_N(r)$ and (b) some reasonable scale-fixing prescription. The latter is needed, since perturbative QCD does not provide any scale-fixing procedure by itself. Driven by such interests, recently we have shown analytically [17] that, based on the renormalon dominance picture, $V_N(r)$ quickly "converges" to a Coulomb+linear potential for $N \gg 1$, up to an $O(\Lambda_{\rm QCD}^3 r^2)$ uncertainty. This was shown (a) by estimating the higher-order terms of $V_N(r)$ using renormalization group (RG), and (b) by adopting a scale-fixing prescription based on the renormalon dominance picture.

Let us explain the scale-fixing prescription (b). According to the renormalon dominance picture, if we choose a scale μ such that $\alpha_S(\mu) \approx 6\pi/(\beta_0 N)$, around this scale, $V_N(r)$ (after cancelling the leading-order renomalon) becomes least μ-dependent and the perturbative series becomes most convergent; cf. Fig. 3. In view of this property, we fix μ such that*

$$\alpha_S(\mu) = \frac{6\pi}{\beta_0 N} \times \xi \qquad (\xi \sim 1). \tag{10}$$

Then we consider $V_N(r)$ for $N \gg 1$ while keeping $\Lambda_{\overline{\rm MS}}$ finite.

Let us first demonstrate our result in the simplest case. We set $\xi = 1$ and the higher-order terms of $V_N(r)$ are estimated using the 1-loop running coupling constant [leading log (LL) approximation]:

$$V_N(r) = -\int \frac{d^3\vec{q}}{(2\pi)^3} \frac{e^{i\vec{q}\cdot\vec{r}}}{q^2} \, 4\pi C_F \, [\alpha_{1L}(q)]_N \,, \tag{11}$$

where $[\alpha_{1L}(q)]_N$ denotes the perturbative expansion of the 1-loop running coupling constant truncated at $O(\alpha_S^N)$:

$$[\alpha_{1L}(q)]_N = \left[\frac{\alpha_S(\mu)}{1 - \frac{\beta_0 \alpha_S(\mu)}{2\pi} \log(\frac{\mu}{q})} \right]_N = \alpha_S(\mu) \sum_{n=0}^{N-1} \left\{ \frac{\beta_0 \alpha_S(\mu)}{2\pi} \log(\frac{\mu}{q}) \right\}^n. \tag{12}$$

Since the scale μ and $\alpha_S(\mu)$ are fixed at each N via the relation (10), $V_N(r)$ is a function of only r and N once $\Lambda_{\overline{\rm MS}}$ is fixed.

*Here, we generalize the prescription of [17] by introducing the parameter ξ, cf. [18].

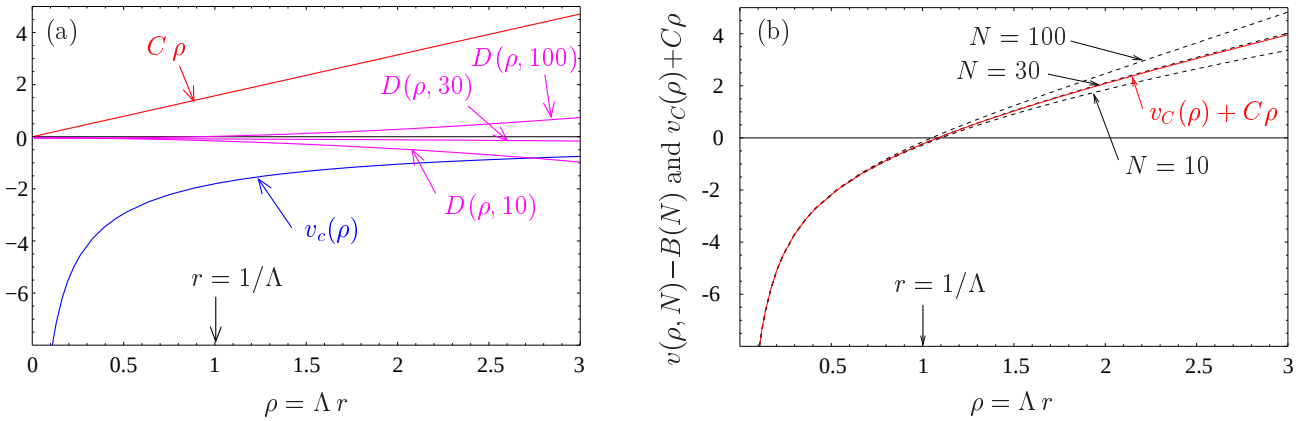

Figure 6: (a) $v_C(\rho)$, $C\rho$ and $D(\rho,N)$ ($N=10,30,100$) vs. ρ. (b) Comparison of $v(\rho,N)-B(N)$ ($N=10,30,100$) [dashed black] and the Coulomb+linear potential $v_C(\rho)+C\rho$ [solid red]. (The latter is hardly distinguishable from the $N=30$ line.)

In the limit $N \gg 1$, $V_N(r)$ can be decomposed into four parts corresponding to $\{r^{-1}, r^0, r^1, r^2\}$ terms (with log corrections in the r^{-1} and r^2 terms):

$$V_N(r) = \frac{4C_F}{\beta_0}\Lambda\, v(\Lambda r, N), \tag{13}$$

$$v(\rho,N) = v_C(\rho) + B(N) + C\rho + D(\rho,N) + (\text{terms that vanish as } N\to\infty), \tag{14}$$

where we rescaled r and V_N by $\Lambda \equiv \mu\,\exp[-2\pi/(\beta_0\alpha_S(\mu))]$. The "Coulomb"[†] [$v_C(\rho)$], linear [$C\rho$] and quadratic [$D(\rho,N)$] parts are displayed in Fig. 6(a); see [17] for the formulas. The constant [$B(N)$] and quadratic [$D(\rho,N)$] parts are divergent as $N\to\infty$, while the "Coulomb" [$v_C(\rho)$] and linear [$C\rho$] parts are finite in this limit. The constant part diverges rapidly, but since it can be absorbed by a redefinition of quark mass in the total energy $E_{\rm tot}(r)$, we will not be concerned with it. The quadratic part is divergent slowly as $D \sim (\rho^2/12)\log N$, and its size is small for $r \lesssim \Lambda^{-1}$ and $N \lesssim 100$ as compared to the Coulomb+linear part; see Fig. 6(a). As a result, when N is increased up to e.g. 10–30, $v(\rho,N)$ quickly "converges" to $v_C(\rho)+C\rho$ at $r \lesssim \Lambda^{-1}$, while it slowly varies as $(\rho^2/12)\log N$, see Fig. 6(b). Note that, although $v(\rho,N)$ in this figure have the form of Eq. (9), they approximate well $v_C(\rho)+C\rho$ at $r \lesssim \Lambda^{-1}$.

If we vary ξ in the scale-fixing prescription Eq. (10), as long as $\xi > 2/3$, we obtain the same Coulomb+linear potential, $v_C(\rho)+C\rho$, whereas $B(N)$ and $D(\rho,N)$ change: for instance, if $2/3<\xi<1$, $D(\rho,N)$ is finite as $N\to\infty$, $D(\rho)=\rho^P\times$ (log-corr.) with $1<P<2$.

We may consider that the constant [$B(N)$] and quadratic [$D(\rho,N)$] parts represent renormalons in $V_{\rm QCD}(r)$. If we perform OPE, these will be (partially) absorbed into $2m_{\rm pole}$ and $\delta E_{\rm US}$ in Eq. (7). On the other hand, the Coulomb+linear part [$v_C(\rho)+C\rho$] may be regarded as a genuine perturbative part, which cannot be absorbed into $2m_{\rm pole}$ and $\delta E_{\rm US}$.

The above result can be systematically improved by incorporating higher-loop effects [next-to-leading log (NLL), next-to-next-to-leading log (NNLL), $\cdots$] into the RG estimate of the higher-

[†]The "Coulomb" part $v_C(\rho)$ contains log corrections at short-distances and its short-distance behavior is consistent with the 1-loop RG equation for the potential.

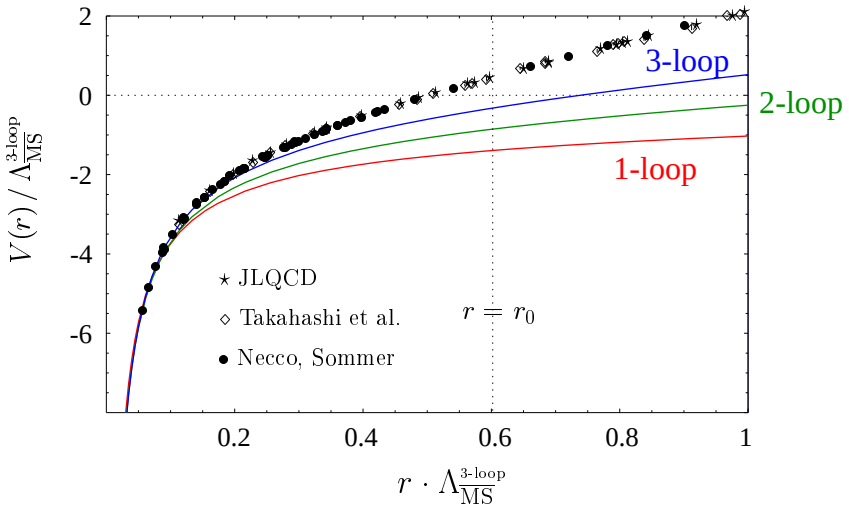

Figure 7: Comparison of the Coulomb+linear potential ($n_l = 0$) with the lattice results in the quenched approximation. 1-, 2- and 3-loop correspond, respectively, to LL, NLL and NNLL approximations in the higher-order estimates.

order terms of $V_N(r)$. Fig. 7 shows the Coulomb+linear potentials corresponding to the higher-order estimates by the 1-loop running (LL), 2-loop running with 1-loop non-logarithmic term (NLL), and 3-loop running with 2-loop non-logarithmic term (NNLL). They are compared with the lattice results. Since the 3-loop non-logarithmic term is not yet known, the 3-loop running case represents our current best knowledge. Up to this order, the Coulomb+linear potential agrees with the lattice results up to larger r as we increase the order.[‡]

The coefficient of the linear potential σr can be expressed analytically. For the 1- and 2-loop running cases, the expressions read

$$\sigma_{\text{1-loop}} = \frac{2\pi C_F}{\beta_0}\left(\Lambda_{\overline{\rm MS}}^{\text{1-loop}}\right)^2, \tag{15}$$

$$\sigma_{\text{2-loop}} = \frac{2\pi C_F}{\beta_0}\left(\Lambda_{\overline{\rm MS}}^{\text{2-loop}}\right)^2 \frac{e^{-\delta}}{\Gamma(1+\delta)}\left[1 + \frac{a_1}{\beta_0}\,\delta^{-1-\delta}\,e^{\delta}\,\gamma(1+\delta,\delta)\right], \tag{16}$$

where $\delta = \beta_1/\beta_0^2$; see [17] for details.

Finally, let us comment on the counter arguments given at the beginning of this section. (1) $V_N(r)$ "converges" to a Coulomb+linear form for $N \gg 1$. (See also discussion in [19].) In fact, already at relatively low orders and at $r \lesssim \Lambda^{-1}$, $V_N(r)$ approximates the Coulomb+linear potential fairly well. (2) Consider a perturbative term $T = \{\frac{\beta_0 \alpha_S(\mu)}{2\pi}\log(\mu r)\}^N$. If we substitute the relation (10) and take the limit $N \to \infty$, it is easy to see that $T \to (\Lambda r)^{3\xi}$. Thus, if we choose a scale μ à la renormalon dominance picture, perturbative terms can converge towards $(\Lambda r)^P$ with some positive power P. Non-analyticity in α_S enters through the relation (10).

5 Conclusions

After cancellation of the leading-order renormalons by using the $\overline{\rm MS}$ quark mass, perturbative uncertainty of $E_{\rm tot}(r) = 2m_{\rm pole} + V_{\rm QCD}(r)$ reduces from $O(\Lambda_{\rm QCD})$ to $O(\Lambda_{\rm QCD}^3 r^2)$ and much more

[‡]The NNLL originating from the ultra-soft scale [20] hardly changes the 3-loop running case displayed in Fig. 7 [17].

accurate perturbative prediction is obtained at $r \lesssim \Lambda_{\rm QCD}^{-1} \sim 1$ fm. Consequently we observe the following:

- $E_{\rm tot}(r)$ up to $O(\alpha_S^3)$ agrees well with phenomenological potentials/lattice results within the estimated uncertainty.
- New physical picture on the composition of the energy of a static $Q\bar{Q}$ system or on the interquark force is obtained: The self-energies of Q and $\bar{Q}$ from gluons with $\lambda_g < r$ increase rapidly as r increases, which makes $E_{\rm tot}(r)$ steeper than the Coulomb potential.
- Our observations are consistent with OPE within potential-NRQCD framework.
- Based on the renormalon dominance picture, the perturbative QCD potential "converges" quickly to a Coulomb+linear potential, which can be computed systematically as we include more terms in the estimate of higher-order terms via RG. In particular, the linear potential can be computed analytically [Eqs. (15,16)]. The Coulomb+linear potential agrees with lattice results up to larger r as we include more terms.

The analyses reported in this paper can be applied to the bottomonium and charmonium spectroscopy in the frame of potential-NRQCD formalism, in which the QCD potential is identified with the leading potential in $1/m$ expansion. Some applications have already been done in our recent works [21]. Furthermore, our analyses provide a basis for (and justification for the error estimates of) the determination of the bottom and charm quark $\overline{\rm MS}$ masses from the $\Upsilon(1S)$ and J/ψ energy levels computed in perturbative QCD [14, 22].

Acknowledgements

Many of the analyses were done in collaboration with S. Recksiegel. The author is grateful for fruitful discussion. He also thanks K. Van Acoleyen and H. Verschelde for discussion.

References

[1] M. Peter, Phys. Rev. Lett. **78**, 602 (1997); Y. Schröder, Phys. Lett. **B447**, 321 (1999).

[2] K. Melnikov and T. v. Ritbergen, Phys. Lett. **B482**, 99 (2000).

[3] A. Hoang, M. Smith, T. Stelzer and S. Willenbrock, Phys. Rev. **D59**, 114014 (1999); M. Beneke, Phys. Lett. **B434**, 115 (1998).

[4] S. Capitani, M. Lüscher, R. Sommer and H. Wittig [ALPHA Collaboration], Nucl. Phys. B **544**, 669 (1999); Erratum ibid. **582**, 762 (2000).

[5] Y. Sumino, Phys. Rev. D **65**, 054003 (2002).

[6] S. Recksiegel and Y. Sumino, Phys. Rev. D **65**, 054018 (2002).

[7] S. Recksiegel and Y. Sumino, hep-ph/0212389.

[8] S. Necco and R. Sommer, Phys. Lett. **B523**, 135 (2001).

[9] A. Pineda, J. Phys. G **29**, 371 (2003).

[10] M. Beneke, Phys. Rept. **317** (1999) 1; Y. Sumino, hep-ph/0004087.

[11] U. Aglietti and Z. Ligeti, Phys. Lett. **B364**, 75 (1995).

[12] M. Beneke and V. Braun, Phys. Lett. **B348**, 513 (1995).

[13] M. Beneke and V. Braun, Nucl. Phys. **B426**, 301 (1994); I. Bigi, M. Shifman, N. Uraltsev and A. Vainshtein, Phys. Rev. **D50**, 2234 (1994).

[14] N. Brambilla, Y. Sumino and A. Vairo, Phys. Lett. **B513**, 381 (2001).

[15] A. Pineda and J. Soto, Nucl. Phys. Proc. Suppl. **64**, 428 (1998).

[16] N. Brambilla, A. Pineda, J. Soto and A. Vairo, Nucl. Phys. **B566**, 275 (2000).

[17] Y. Sumino, Phys. Lett. **B571**, 173 (2003).

[18] M. Beneke and V. Zakharov, Phys. Rev. Lett. **69**, 2472 (1992); K. Van Acoleyen and H. Verschelde, hep-ph/0307070.

[19] V. Zakharov, hep-ph/0309178.

[20] A. Pineda and J. Soto, Phys. Lett. **B495**, 323 (2000).

[21] S. Recksiegel and Y. Sumino, Phys. Rev. D **67**, 014004 (2003); hep-ph/0305178 (*to appear in Phys. Lett. B*).

[22] N. Brambilla, Y. Sumino and A. Vairo, Phys. Rev. **D65**, 034001 (2002).